iScience

CellPress
OPEN ACCESS

Article

The severity of dry and hot climate extremes and their related impacts on vegetation in Madagascar

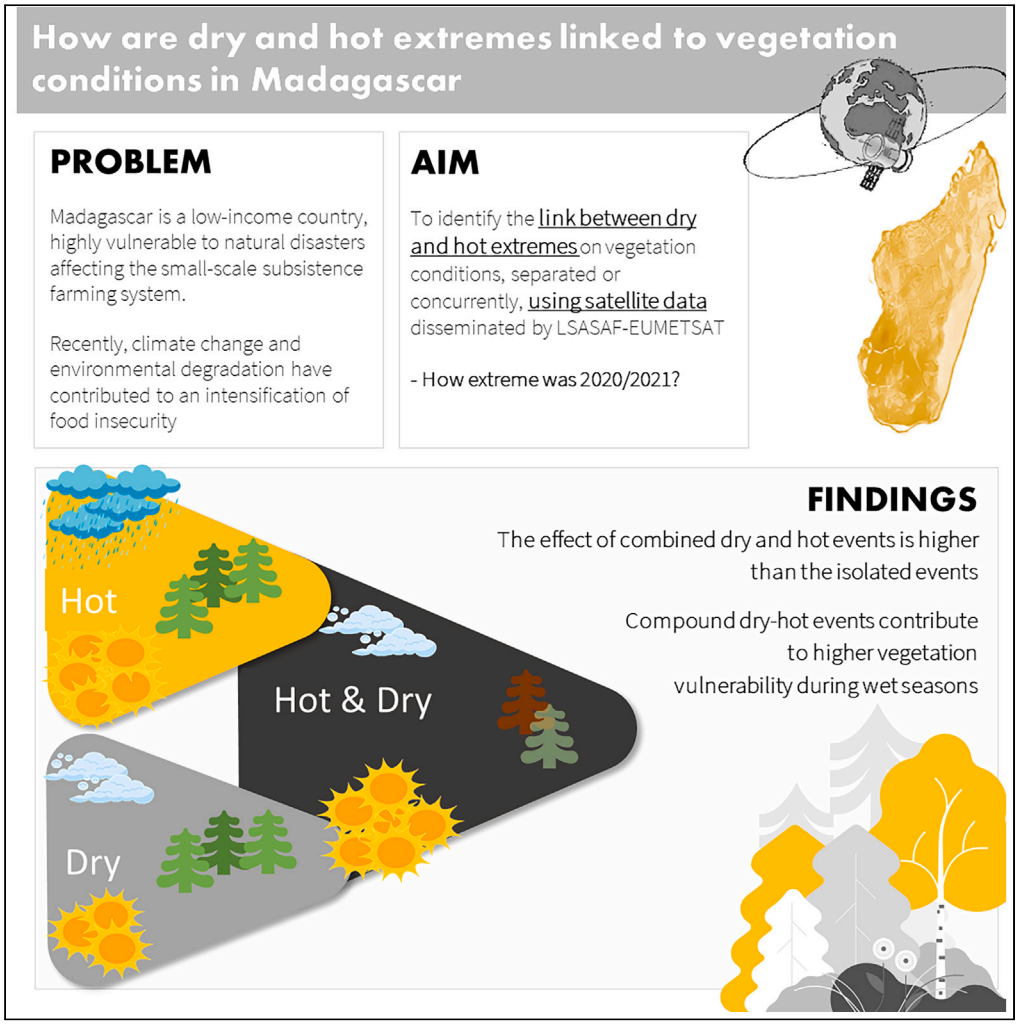

Célia M. Gouveia, Mafalda Silva, Ana Russo

celia.gouveia@ipma.pt

Highlights

The effect of combined dry and hot events is higher than the isolated events

The link between vegetation, drought, and hot events is evident in southern Madagascar

Compound dry-hot events are related to vegetation vulnerability during wet seasons

The cooccurrence seems to be privileged by the magnitude of the events

Gouveia et al., iScience 27, 108658
January 19, 2024
https://doi.org/10.1016/j.isci.2023.108658

iScience

CellPress
OPEN ACCESS

Article

The severity of dry and hot climate extremes and their related impacts on vegetation in Madagascar

Célia M. Gouveia,[1,2,3,*] Mafalda Silva,[1] and Ana Russo[2]

SUMMARY

Madagascar is a low-income country, highly vulnerable to natural disasters affecting the small-scale subsistence farming system. Recently, climate change and environmental degradation have contributed to an intensification of food insecurity. We aim to monitor the link between dry and hot extremes on vegetation conditions, separated or concurrently, using satellite data, such as LST, ET, ET0, and FAPAR products from SEVIRI/MSG disseminated by LSASAF-EUMETSAT. The analysis was made for a long record from 2004 to 2021, focusing on the extreme seasons of 2020 and 2021. Results highlight the higher impact of combined dry and hot events when compared with isolated events, with a strong response of vegetation in the southern part of Madagascar. Results point to the added value of using the recent data records from geostationary satellites with high temporal resolution and updated in near real-time, to early detect, monitor, and characterize the impact of climate extremes on vegetation dynamics.

INTRODUCTION

Madagascar is a mountainous island located in the Southwestern Indian Ocean, off the South-Eastern coast of Africa, extending over 580 km from east to west and 1600 km from north to south (Figure 1). With a gross domestic product of USD 422 per capita (around 70% of the population lives on less than USD 1.90 a day), Madagascar is a low-income country.[1] The high vulnerability to natural disasters, associated with the prevalence of the rainfed small-scale subsistence farming system, also susceptible to natural disasters, has played a crucial role in the low human development achieved in the last decades. Madagascar is among the 10 countries most affected by disasters[2] and is considered the most cyclone-exposed country in Africa.[3] Madagascar is therefore highly susceptible to the occurrence of extreme weather and climate events, which have a direct impact on ecosystems.[4–10] Madagascar was affected during the last years by extreme droughts at levels not seen in four decades, which led to crop failures and widespread food shortages[11] and drought-induced deforestation.[7] The Grand Sud region has been affected by successive drought events in the 2019/2020 and 2020/2021 rainy seasons.[3] The successive dry conditions in agriculture were disastrous, forcing people to adopt desperate survival measures, such as eating locusts, raw red cactus, or wild leaves.[11] Since late 2020s, dozens of starvation deaths have been recorded in Madagascar,[12] and more than 1.1 million people—out of a population of about 27 million—are food insecure.[11] This period of years of drought, associated with intense deforestation, poverty, and population growth, has led the country to change to a desert-like country, and it is expected to worsen due to climate change and temperature warming. According to the most recent climate projections,[13] a robust increase in the annual mean temperature ranging from 0.9°C to 1.2°C is projected in the 1.5°C global warming level, with the west and southwestern parts of the island displaying the highest rise in temperature. On the other hand, the changes in rainfall are not so clear and show larger uncertainties, depending on the location, the months within the rain season, and the warming level. Projected decreases in rainfall associated with projected increases in the length of the dry periods can cause supplementary stress on already vulnerable livelihoods in southern Madagascar. Additionally, projected temperature increases could disrupt even more certain micro-climates and lead to significant changes to local farming systems, with implications for food security.[14] Nevertheless, it is important to stress that, according to the IPCC's recently published 6th Assessment Report that surveyed the evidence from attribution analyses, the projected changes in precipitation, heatwaves, and droughts have different confidence levels.[15] The expected increase in heat extremes has low confidence on human attribution due to low agreement, whereas high precipitation and drought changes have limited data/literature and low agreement, respectively. Following the Framework's recommendations, the relation between different cooccurring or consecutive extreme events has been addressed on a regional to global basis, namely focusing on the effect of antecedent drought conditions on the occurrence of temperature extremes.[16–23] The role of spring precipitation deficits increased solar radiation and warming in amplifying the high-temperature anomalies in extreme summers due to soil moisture depletion has been highlighted in several studies.[24] Additionally, the occurrence of preceding drought conditions has been identified to constrain in certain regions subsequent hot events.[16,18]

[1]Instituto Português do Mar e da Atmosfera, Lisboa, Portugal
[2]Universidade de Lisboa, Faculdade de Ciências, Instituto Dom Luiz (IDL), 1749-016 Lisboa, Portugal
[3]Lead contact
*Correspondence: celia.gouveia@ipma.pt
https://doi.org/10.1016/j.isci.2023.108658

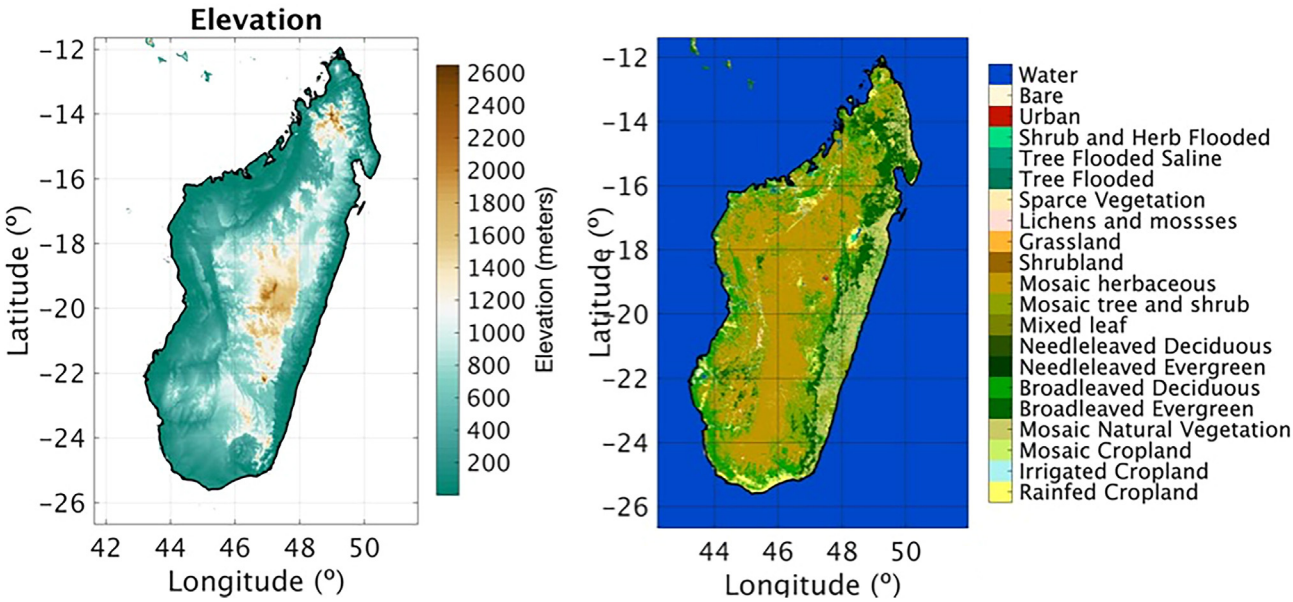

Figure 1. Study area: Madagascar island

(A) Elevation in meters.

(B) Land cover map from ESA-CII land cover product for 2018.

Apart from the documented association between droughts and heat extreme events in certain parts of the world, their influence on vegetation activity has been also analyzed during the last years.[5,24–28] Previous studies pointed out that the depletion of soil water content amplifies high temperatures due to the increase of sensible heat fluxes,[29] leading to a consequent reduction in the transpiration and photosynthetic activity of vegetation,[30] which on the other hand can lead to severe wildfires and consequently to considerable economic, social, and environmental damages.[31] Moreover, the land-atmosphere-vegetation interplay can occur with different levels of damage, even for low-intensity extremes,[32] and its highly dependent on the land cover.[25,33,34] Despite the scientific progress to date regarding the analysis of compound extreme events, the full perception of the association between heatwaves and droughts and its impacts on vegetation are still a challenge, particularly in South America and Africa[20,35] where this compound framework approach is still incipient.

This case study aims to address three important caveats identified in the literature, namely (1) the lack of published works adopting a compound framework in African regions, (2) the analysis of the relation between the compound dry and hot events with the vegetation conditions in Madagascar, and finally, (3) the capability of doing this type of analysis using satellite-derived near-real-time (NRT) datasets. In order to accomplish the proposed goals, remote sensing information between 2004 and 2021 will be used. The ability of satellite data to monitor the response of vegetation to single dry and heat extremes and the cooccurrence of these extremes in NRT is shown. The extreme drought and heatwave conditions of 2020 and 2021 are analyzed, and their relationship with vegetation conditions over Madagascar is modeled using satellite information about vegetation, evapotranspiration, and land surface temperature.

RESULTS

Monthly means of Land Surface Temperature (LST), Evaporative Stress Index (ESI), and Fraction of Absorbed Photosynthetically Active Radiation (FAPAR) (see STAR Methods section) were computed considering the reference period from 2004 to 2021 (Figures 2, 3, and 4). LST values are higher in west and south regions, reaching values around 35°C in November and December. On the other hand, LST values are lower in east coast and highlands with monthly mean values around 10°C from June and July (Figure 2). Moreover, lower ESI values are observed in the southern sector from April to December, showing more extreme dry values affecting a widespread region from June to November. The central highland region also shows low values of ESI from July to October, although not so extreme (Figure 3). The monthly spatial patterns of LST and ESI are compatible with the wet and warm versus cool and dry seasons, i.e., hot and rainy season (high LST and ESI) from November to April and cooler and dry season from May to October (low LST and ESI) (Figure 5). The spatial patterns of FAPAR are also compatible with the previous spatial patterns of ESI and LST, showing higher photosynthetic activity in regions and months characterized by wet and mild conditions. Low values of FAPAR are observed from May to December, with lower values from August to November over west, inland, and south regions, typical of grassland, woodland, and dry forest types. High vegetation activity is observed over the entire island from February to April and remains high during the whole year in the east coast, which is dominated by tropical rainforest (Figure 4). It should be stressed that higher vegetation activity occurred between January and April, coincident with the hot months if there is water availability but is lower between September and November when even higher temperatures are observed in the dry months (Figure 5).

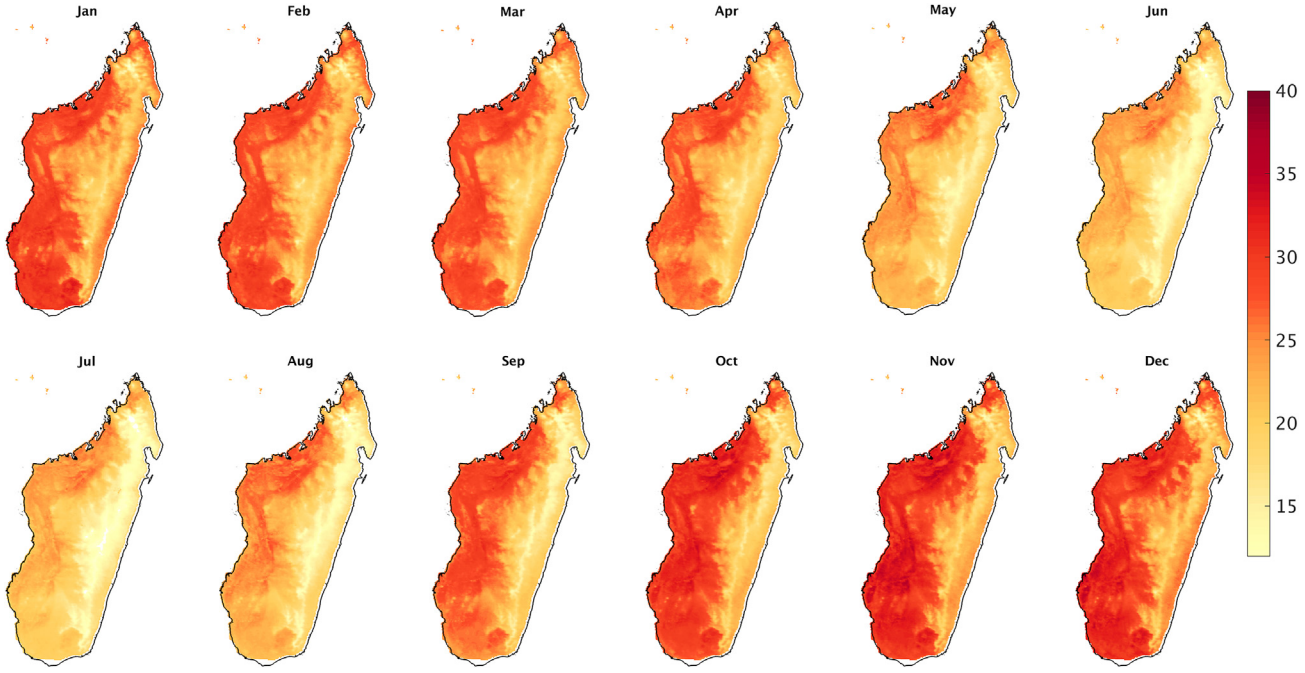

Figure 2. LST monthly means over Madagascar from 2004 to 2021 (Units: °C)

The occurrence of hot and dry extremes observed in 2020 and 2021 is depicted in Figures 6, 7, and 8. Strong positive monthly LST anomalies (up to 6°C) are recorded in February, November, and December 2020 and January, February, and December 2021. Nevertheless, less intense, already positive monthly LST anomalies (around 2°C) are spread over the island except for eastern coastal areas in some months (Figure 6, top panel). Negative anomalous values of LST are very rare and sparse in the island during 2021, but preferentially over coastal and northern regions. On the other hand, some consistent spatial patterns of negative anomalies of LST were observed in January 2020 in coastal and northern regions and over east coastal areas from February to July and October and December of 2020 (Figure 6, bottom panel).

The dry patterns in 2020 and 2021, as obtained from ESI negative anomaly values, are also obvious (Figure 7). Strong and consistent negative spatial patterns of ESI are found in the 24 considered months with higher negative values over southern and southwestern regions. Negative ESI anomalies are observed from January to June and November and December of 2020 mainly over southern and western regions. Some isolated positive anomalies are also found mainly from June to October over northern and central highland regions (Figure 7, top panel). The spatial patterns of negative ESI anomalies are stronger in 2021, in particular in January, April, May, November, and December affecting once again the southern and western sectors. Consistent and strong positive patterns are found in the North and central highlands from April to August and over the north and eastern coastal regions from September to December of 2021 (Figure 7, bottom panel).

The impact of climate extremes on vegetation activity observed in 2020 and 2021 is depicted in Figure 8. Negative anomalies of FAPAR resulted from lower than usual canopy's ability to absorb radiation for photosynthesis and lower than usual photosynthetic activity and biomass production. Vegetation activity is also strongly dependent on water availability. Negative anomalies of FAPAR are observed in most of the months of the two years, except for September and October 2021 over the entire island and January to March both in 2020 and 2021 in the Central and Northern sectors (Figure 8). Strong and consistent spatial patterns of strong negative anomalies of FAPAR are found mainly in southern regions, although some hotspots over inland lowland and northern regions, namely in April and October 20202 and March to June 2021. The severity of the impact of hot and dry events is stronger from December 2020 to March 2021 and December 2021 over the southwestern and southern regions of Madagascar Island (Figure 8, bottom panel).

The persistence of the climate extremes (dry and hot conditions) and their relationship with vegetation are linked to the long-lasting duration of the events. The number of months presenting negative anomalies of ESI (lower than the 20th percentile: −0.05) and positive anomalies of LST (higher than 80th percentile: 1°C) during the two years are computed and shown in Figure 9 (left and central panels). A large and spread region ranging from 10 to 22 months of high positive anomalies of LST is located in the west, central highlands, and southern sectors. The lowland areas close to the east coast, from south to north, exhibit very few months with positive LST anomalies (lower than five months) in the two consecutive years (Figure 9, left panel). This region also shows a few months with negative anomalies of ESI, although some inland east areas with around 10 months of dry conditions. On the other hand, a sharp contrast between the north and south sectors was found with a pattern with less than five dry months in the north and another with more than 30 dry months in the southern sector. The high number of drought months in the south and southwestern sectors are conspicuous. Areas ranging from 10 to 20 dry months over the lowland west region are also observed (Figure 9, central panel).

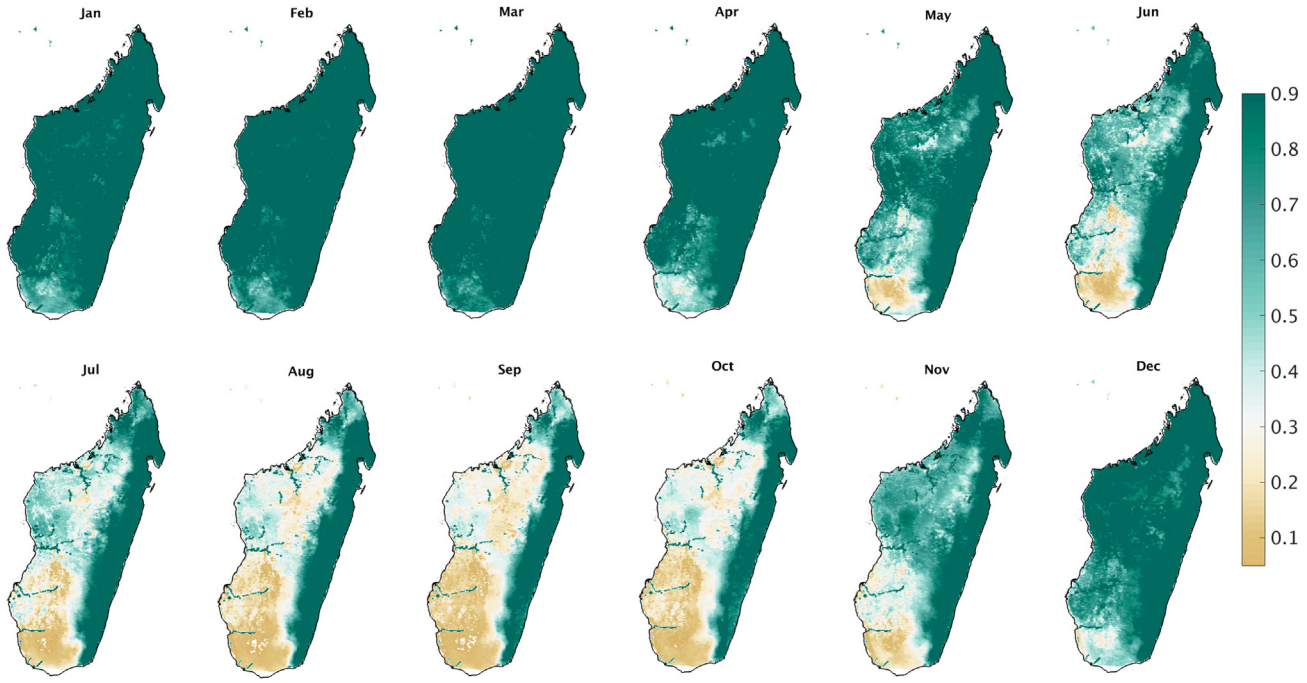

Figure 3. ESI monthly means over Madagascar from 2004 to 2021 (Units: dimensionless)

The percentage of Madagascar island area (%) affected for more than 9, 14, and 18 months by individual stressing conditions of dry, hot, vegetative stress (veg-) or by compound events of hot and dry, hot and vegetative stress, dry and vegetative stress, and hot and dry and vegetative stress are presented in Table 1. More than half of the island area was stricken by more than nine months of hot conditions, followed by around 40% being affected by drought for more than nine months for two years, contrasting with the one-fifth of the area showing stressed vegetation. Although a higher percentage of the island (~1/3) was affected by hot and dry conditions, the percentage of area affected by stressed vegetation and other weather extremes, isolated or compound, remains around 1/5 of the island. On the other hand, the percentage of area affected by longer periods of extreme heat decreased to 21% during more than 14 months and 5% when more than 18 months are analyzed, whereas the decrease is less accentuated in the case of persistent drought and vegetative stress (22% and 5% for drought and 9% and 4% for vegetation). The decrease of area affected for the compound events observed for a longer period is similar to the ones described for the persistence over nine months.

The regions exhibiting more than nine months with hot and dry surface conditions are represented in black in Figure 9 (right panel). The areas showing dry conditions for more than nine months are represented in green, and the pixels struck by heat conditions for more than nine months are represented in red. A large pattern of pixels coaffected by more than nine months of dry and heat conditions are observed in black (Figure 9, right panel). It should be stressed that the cooccurrence of nine months of negative (positive) anomalies of ESI (LST) does not require a contemporaneous occurrence. Results show a large area coaffected by hot and dry conditions in the two-year period over South and the southwestern sectors with some hotspots in west lowland regions. A large area affected solely by hot conditions is observed in central highland areas (Figure 9, right panel).

The persistence of vegetative stress conditions in Madagascar is assessed by computing the number of months presenting negative anomalies of FAPAR (lower than the percentile 20: −0.03) (Figure 9, left panel). A large spatial pattern of more than 18 months (out of 24) with negative anomalies of FAPAR is observed over the southern sector of the island, with some hotspots in southwest and west coastal regions and southern highlands. On the other hand, the east coastal region, the west, north, and central highlands show a low number of months with negative anomalies of FAPAR, whereas the east region seems not to be affected by either hot or dry conditions (Figure 9, left panel).

With the aim to associate the areas exhibiting several months of lower vegetation activity with the areas affected by concurrent heat and dry conditions, the pixels with more than nine months of negative anomalies of FAPAR are selected. Figure 10 (right panel) shows the scatterplot of the number of months presenting heat (LSTsum, y axis) and dry (ESIsum, x axis) conditions for those selected pixels showing persistent vegetative stress (the colors of pairs [ESIsum, LSTsum] in the plot). Results show that the pixels corresponding to pixels with the high number of months with vegetative stress (ranging from 15 [yellow] to 24 [red] months) correspond to pixels with more than 18 dry and heat months (ESIsum and LSTsum higher than 18). Some pixels presenting long-lasting vegetative stress are associated only with persistent dry conditions (ESIsum higher than 18 months and LSTsum around 5 months). Results highlight the persistence of dry and hot conditions and the stronger and larger impact on vegetation activity of the composite occurrence compared with the isolated occurrence of dry conditions.

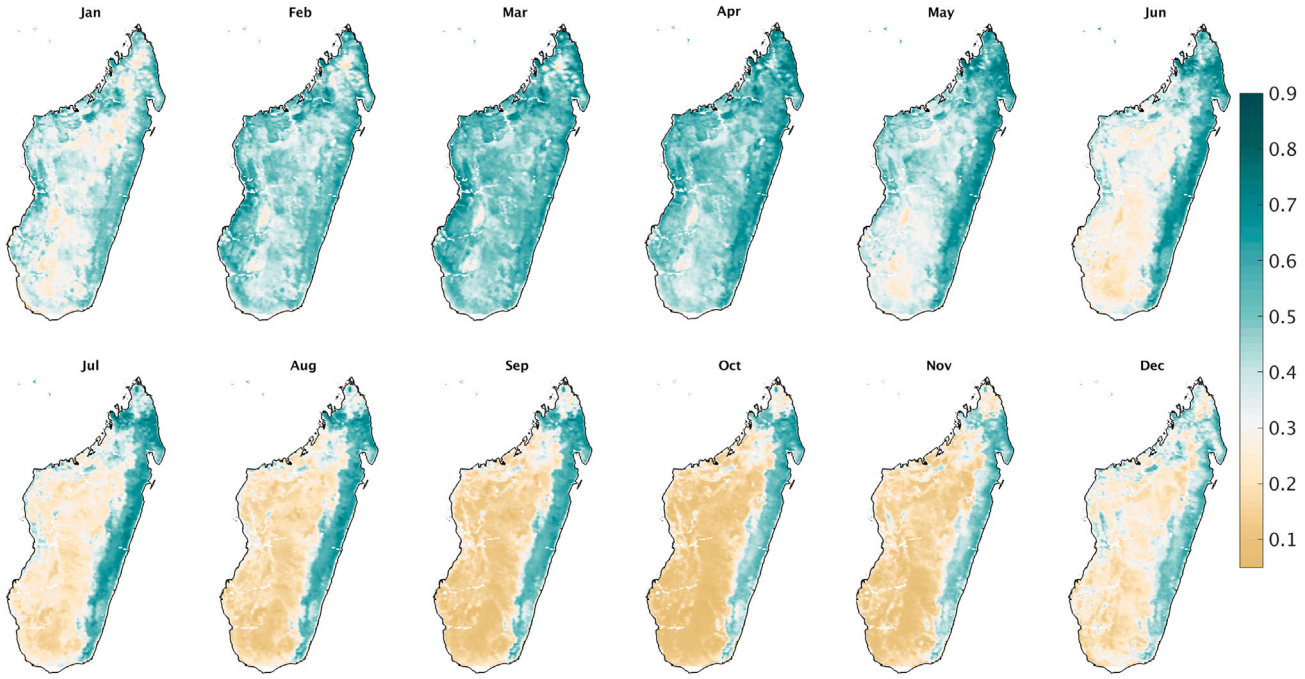

Figure 4. FAPAR monthly means over Madagascar from 2004 to 2021 (Units: dimensionless)

Figure 11 represents the temporal evolution, from 2004 until 2021, of FAPAR anomaly values averaged over pixels coded in Figure 9 (right panel) as persistent dry (green), hot (red), and hot and dry (black). The larger impact of persistent hot and dry conditions on vegetation activity, as obtained by FAPAR anomaly values, is notorious. Persistent negative FAPAR anomaly values are observed from the end of 2019 until the end of 2021, with few exceptions in the beginning and a few months before the end of 2021. The annual accumulation of FAPAR anomaly values averaged over pixels coded as persistent dry (green), hot (red), and hot and dry (black) are presented in Figure 11, bottom panel. According to the temporal evolution presented (top panel), the sum of spatial averaged negative anomaly values for hot and dry pixels is conspicuous during 2020 and 2021, being a record since 2004. The sum of spatial averaged negative anomaly values for hot and dry pixels in 2018 and 2010 is also evident. On the other hand, the evolution of strong negative anomalies for hot and dry pixels observed from the end of 2014 and the beginning of 2015 (top panel) does not correspond to a significant annual sum of negative FAPAR anomalies (bottom panel), as they distributed by two years (2014 and 2015) with normal and positive FAPAR anomalies.

It should be stressed that the exceptionality of the impact on vegetation activity is related not only to the persistence of vegetative stress but also to the magnitude of impact, as seen by the magnitude of the averaged values of monthly anomalies of FAPAR (Figure 11, top panel) and by the sum of negative averaged values that persisted during the annual assessment (Figure 11, bottom panel). The persistence and magnitude of the negative annual averaged FAPAR anomaly values are much larger for hot and dry, followed by dry, and finally by hot conditions. The strong negative vegetation behavior observed in 2009/2010 and 2014/2015, despite presenting high severity (magnitude), is not very persistent (three or four months). The greater impact of dry and hot conditions is not evident when compared with dry and hot separately (Figure 11, top and bottom panels), in particular in 2014/2015 and 2017/2018. This feature could be related to the criterion used here to select pixels that relied on the persistence of the vegetative stress conditions in the two-year period of 2020 and 2021. Another interesting feature is the persistent low vegetation activity observed over the pixels, showing hot and dry conditions in 2020 and 2021, also during 2018, which accounts for almost 36 months in four years (48 months) with vegetative stress during the last four years (48 months), which may represent strong impacts for crop production and food security.

DISCUSSION

Madagascar is among the top 10 countries most affected by natural disasters,[2] where massive cyclonic storms take the lead in terms of impacts.[3] Nevertheless, their dry counterparts have been hitting frequently the Grand Sud region in the last years (e.g., 2019/2020 and 2020/2021 rainy seasons' droughts[3]), leading to crop failures and widespread food shortages.[11] These successive extremely dry years have had tremendous impacts on the agriculture sector, forcing people to starve and rely on scarce and not common food supplies.[11,12] These stressful conditions are expected to worsen in the future years due to global warming, with temperatures being projected to increase in Madagascar between 1.1°C and 2.6°C by 2065.[14] Projected decreases in rainfall associated with estimated increases in the length of the dry periods are expected to put further pressure on already vulnerable people and ecosystems, particularly in southern Madagascar.[14]

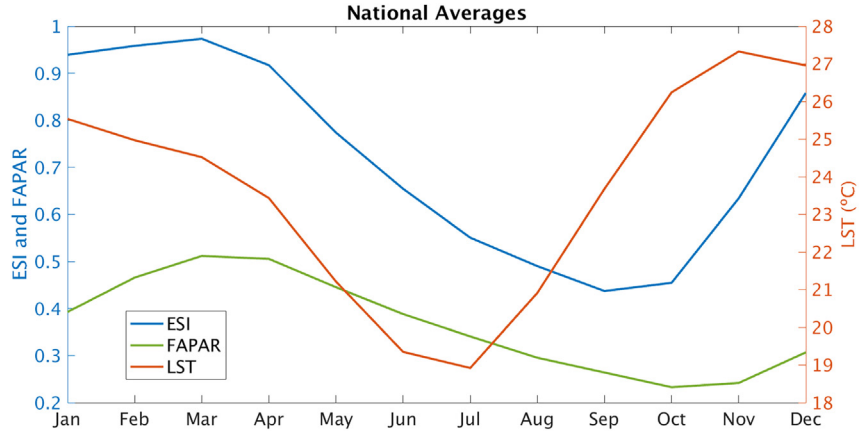

Figure 5. Annual cycle of spatially averaged values over Madagascar island of LST, ESI, and FAPAR considering the period from 2004 to 2021

Regardless of the already identified impacts of extreme events, the occurrence of compound events and the accountability of their impacts is still a challenge, particularly in certain areas of the globe, like Madagascar. In this sense, the present case study aimed to contribute to improving the knowledge of the occurrence of dry and heat extremes in Madagascar and its relation with vegetation conditions using remote sensing information between 2004 and 2021. Special attention was devoted to the occurrence of compound events, and a detailed analysis of the exceptional extreme drought and heatwave conditions of 2020 and 2021 was performed.

The results obtained in this work indicate that using parameters obtained exclusively by remotely sensed data can provide helpful information about the occurrence of extreme dry and hot conditions and associated vegetation conditions. This work highlights that it is possible to evaluate the cooccurrence of extreme events (compound or individual) and vegetation conditions at a regional scale based solely on low-resolution remotely sensed observations that are easily and freely accessible. The results show that the recent low-resolution data records from geostationary satellites, now available for almost 20 years, provide important information to early detect, monitor, and characterize the impact of climate extremes on vegetation dynamics and crop production, in particular considering their high temporal resolution, low number of missing values, and dissemination in NRT. Although low-resolution remote sensing observations have been shown to provide information about vegetation in previous studies, their availability on NRT and their improved quality and length have a significant impact on studies in certain areas like Madagascar. Therefore, the approach presented in this study is a valuable and easy tool for agricultural monitoring and for estimating vegetation conditions associated with climate extremes, such as drought and heatwaves. Previous studies applying remote sensing approaches, relying on a variety of indices, were successfully applied to other African regions (e.g., [36–39]). Nevertheless, these studies do not account for the interplay between different stressors, namely between drought conditions and heat stress. To the best of our knowledge, the present study constitutes a first attempt at analyzing the combined effect of dry and hot conditions and their impact on vegetation in Madagascar.

Our results highlight that hot and dry conditions are highly dependent on altitude and distance to the coastline, following an NW to SW gradient. Namely, LST values are higher in the west and the south regions, and ESI values are lower in the southern sector. As it was identified for the Mediterranean area and for the Balkans by Russo et al., [18] the presence of dry conditions in the months preceding the warmer months is of high importance to the occurrence of extremely hot events. This association suggests a strong relationship between precipitation deficits and the following occurrence of hot extremes also identified over other parts of the globe, [16] namely in America [40] and India. [41]

We find a synergy between the occurrence of extreme hot and dry events and vegetation conditions over several areas following similar patterns to the one identified for hot and dry extremes, which is a cause of concern, as the prospect of more frequent and intense compound events like droughts and heatwaves is projected to increase in the future. [14] When the analysis is particularized for the extreme years of 2020 and 2021, strong positive LST anomalies (up to 6°C) are recorded during the wet seasons (February, November, and December 2020 and January, February, and December 2021). This situation was intensified by the presence of long-term drought conditions in more than 9 months in 2020 and 10 months in 2021 over southern and western regions. Conversely, strong wet conditions were found in the north, central highlands and eastern coastal regions. These extreme dry and hot events had an expressive impact on vegetation, particularly in the southern region and during the 2020 and 2021 dry seasons (from April to October 2020 and March to June 2021). However, the severity of the impact of hot and dry events was stronger during the wet season (from December 2020 to March 2021), which was linked to the long-lasting duration of the events.

Although using satellite data only available from 2004 to the present, our work was able to identify several drought events with significant impacts on vegetation activity over southern Madagascar. Droughts are frequent in the region, namely considering the six severe events in the last decade, often with total loss of crops and widespread food insecurity. [42] Despite the relative adaptation of the population to low groundwater and river levels, however, the higher temperatures in recent years have exacerbated this deficit.

The higher impact of composite hot and dry extremes on vegetation activity in 2020 and 2021 over the southern region is evident and consistent with the huge impacts in the agriculture sector, namely the subsistence farming with traditional methods, which forced 80% of

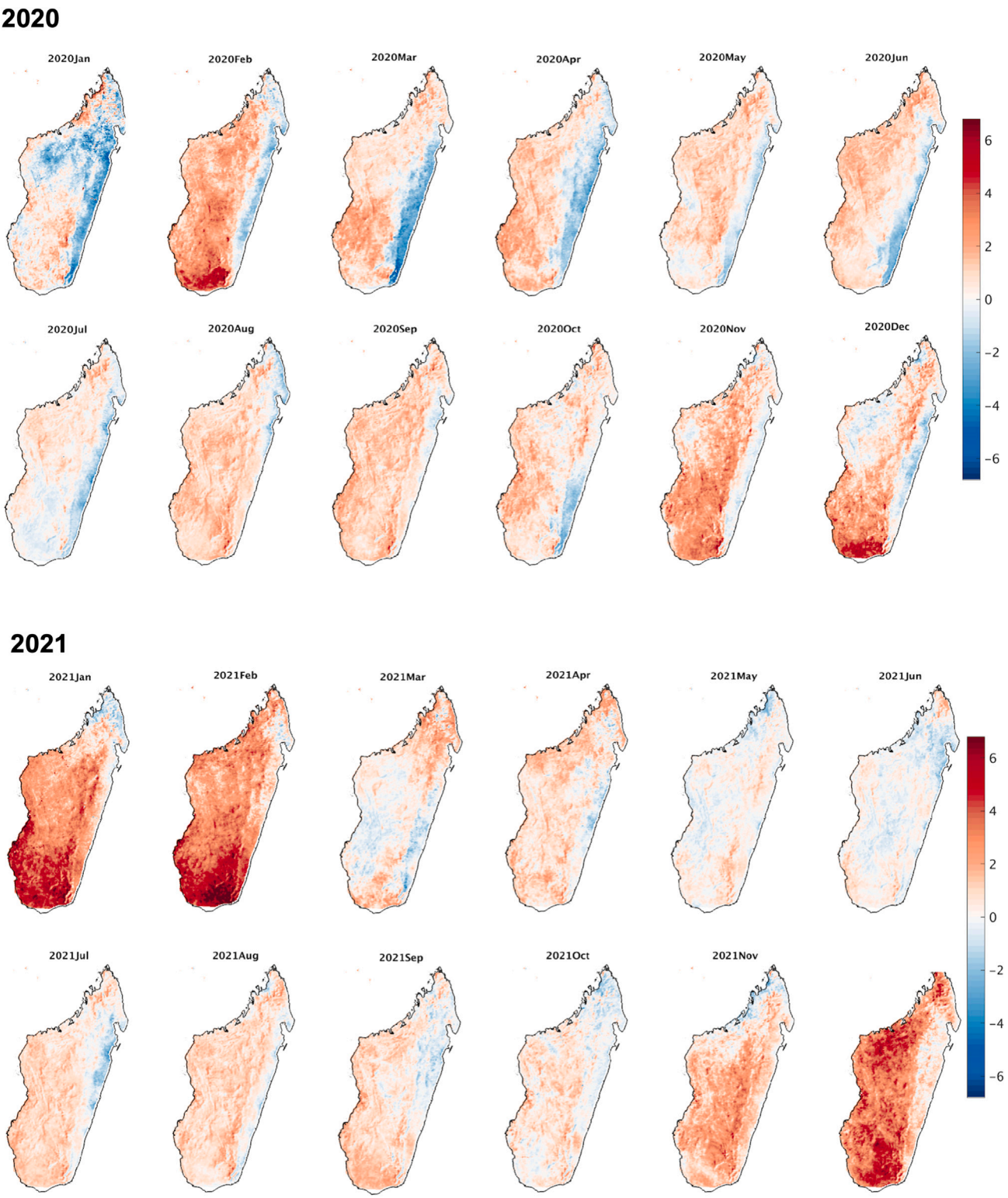

Figure 6. LST monthly anomalies for 2020 (top) and 2021(bottom) over Madagascar

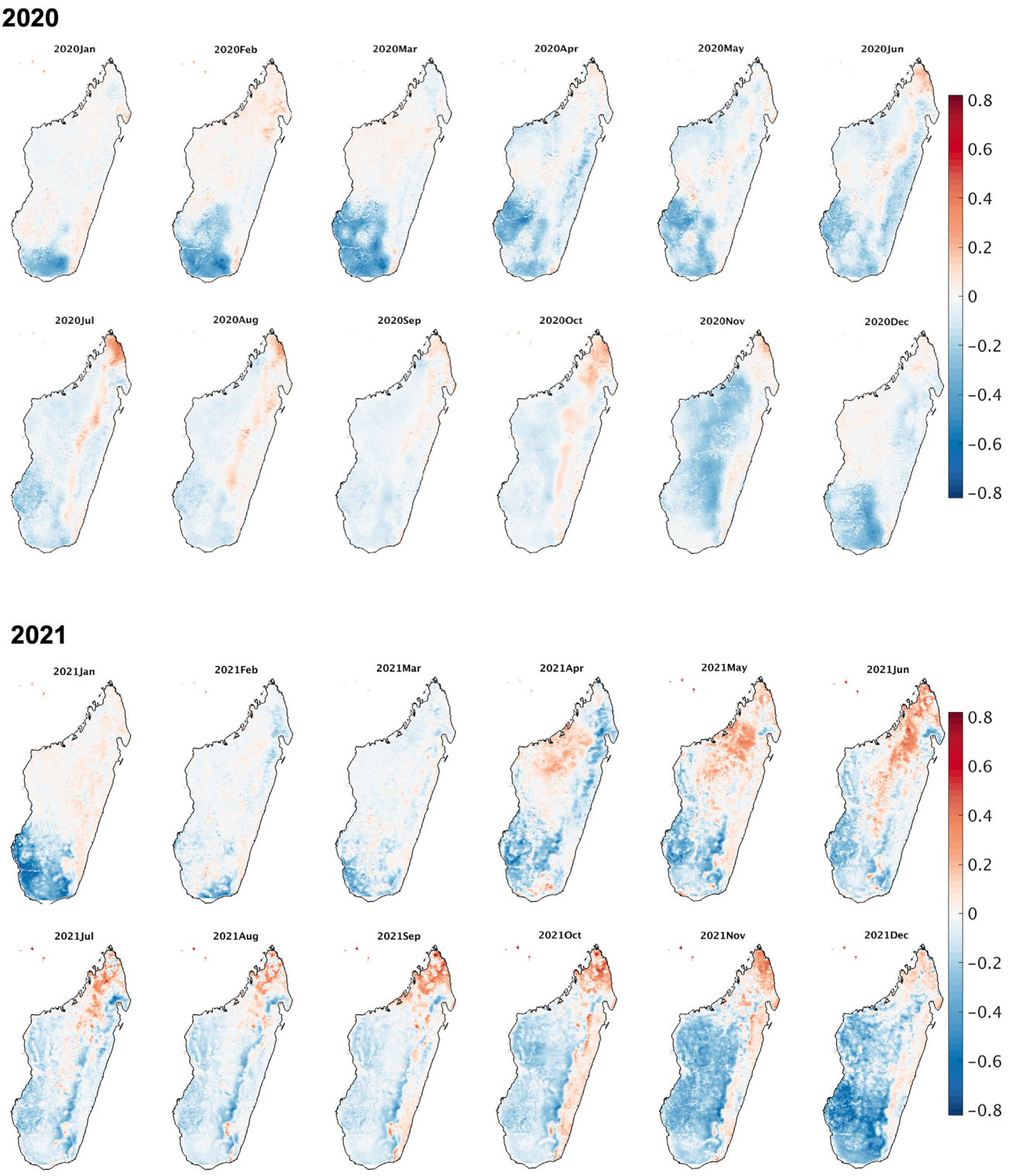

Figure 7. ESI monthly anomalies for 2020 (top) and 2021(bottom) over Madagascar

the population to desperate survival measures.[42] Our results are in accordance with the exceptional character of the drought event that was called the worst drought in 30 years, affecting agriculture for three consecutive years,[43] mainly considering the water deficits occurred during the planting seasons, causing consecutive failed harvest.[42] Although the largest relation of compound dry and hot extremes with vegetation

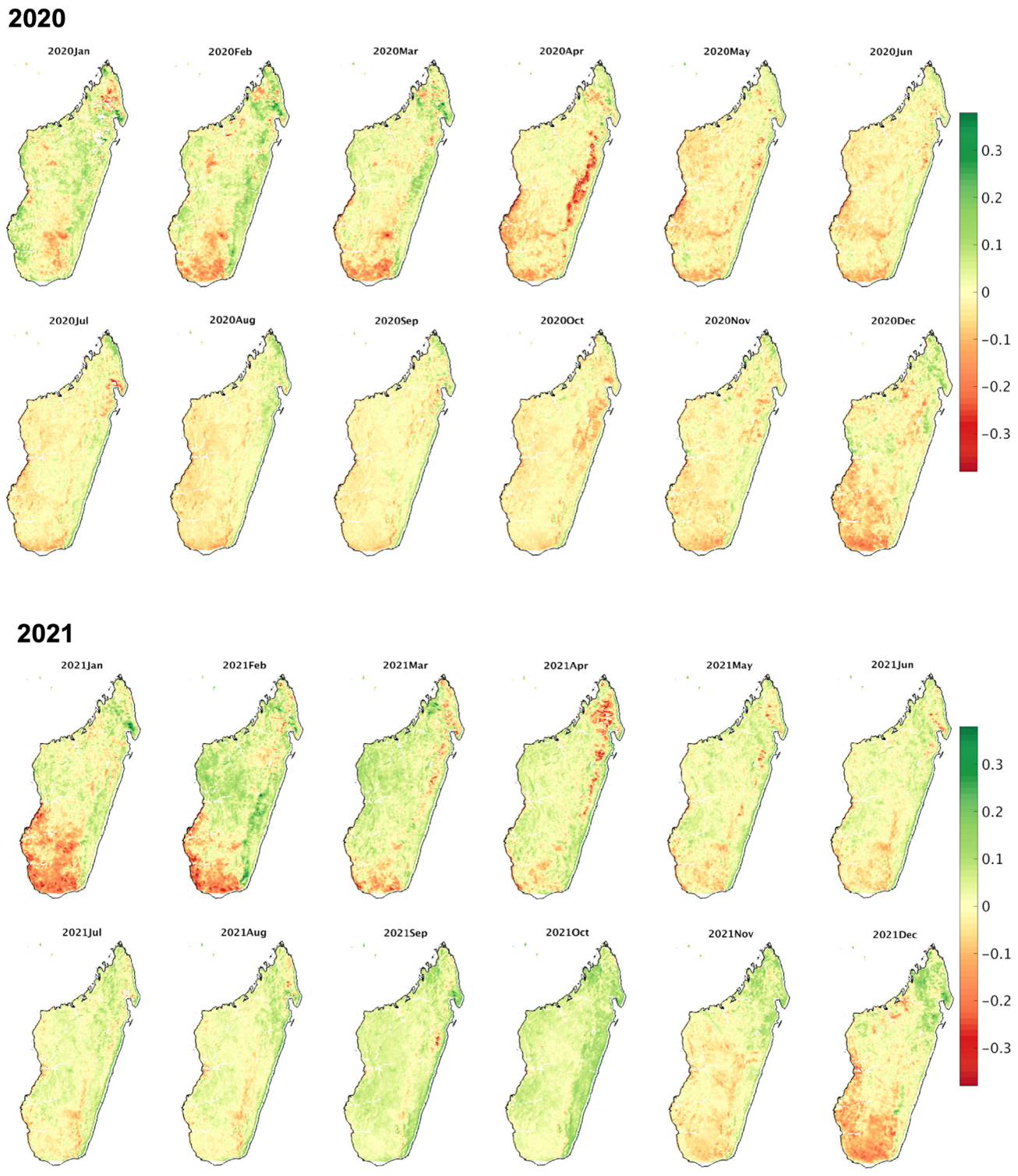

Figure 8. FAPAR monthly anomalies for 2020 (top) and 2021(bottom) over Madagascar

was seen in the southern regions, some hotspots were also identified in the western lowland regions. It is important to highlight that the cooccurrence and persistence of dry and hot conditions have a stronger and larger influence on vegetation activity when compared with the isolated occurrence of dry conditions.

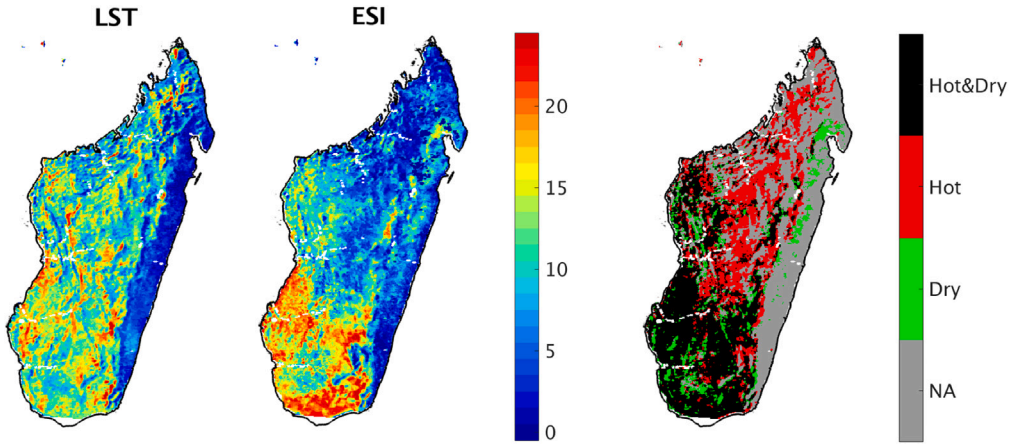

Figure 9. The number of months with LST anomalies higher than 1°C (left) and ESI anomalies lower than −0.05 (middle) over Madagascar for the two years of 2020–2021

Spatial pattern of pixels affected by more than nine months of negative anomalies of ESI (dry) and positive anomalies of LST (hot) and cooccurrences of more than nine months of negative anomalies of ESI and positive anomalies of LST (hot and dry). Cooccurrence does not require a contemporaneous occurrence.

Limitations of the study

Although Madagascar has been facing prolonged drought, which is expected to continue to worsen in the future years due to climate change, a new attribution study,[44] led by a team from the World Weather Attribution (WWA) network, finds that although climate change may have slightly increased the likelihood of this reduced rainfall, the effect is not statistically significant. Thus, climate change is not the main driver of the recent food insecurity in Madagascar. One important anthropogenic factor that contributes to food insecurity is the low level of mineral and organic fertilizers utilization and insufficient technological knowledge that directly contributes to the low yields obtained.[44] This is one of the caveats of this work, as this study focuses on the response of vegetation to two climatic factors without considering the effects of non-climatic factors, which in the case of Madagascar have been reported to have a huge impact (e.g., irrigation, fertilization, and overgrazing practices)[44,45] and other natural disturbances (e.g., desertification, wildfire, and pest outbreaks).[46]

Another one of these caveats is that we do not differentiate among land covers nor crops. All in all, these factors can lead to drastic effects that can contribute to the intensification of impacts when compound events occur. Finally, we present evidence based on remote sensing data of the cooccurrence of these extremes, but based on this approach we are not able to quantify the impacts of hot and dry extremes on vegetation conditions. In future, the analysis of different land occupations and human practices and also the quantification of the impacts should be included and analyzed.

Conclusions

In general, climate extremes have a significant impact on different ecosystems. In this study, a remote sensing approach is applied for exploring the relationship between compound dry-hot events with vegetation conditions in Madagascar.

The main findings are summarized as follows.

(1) The combined effect of dry and hot events in vegetation has a higher impact than the isolated occurrence of events.

Table 1. Percentage of Madagascar island area (%) affected by more than 9, 14, and 18 months of dry, hot, vegetative stress (veg-), hot and dry, hot and vegetative stress, dry and vegetative stress, and hot and dry and vegetative stress

	Percentage of Madagascar island (%)		
	>9	>14	>18
Dry	42.7	21.4	9.7
Hot	55.9	21.8	5.1
Veg-	22.2	9.3	3.5
Hot & dry	35.0	10.6	1.9
Hot & veg-	20.2	5.4	1.0
Dry & veg-	21.0	8.1	2.7
Hot & dry & veg-	19.3	4.7	0.8

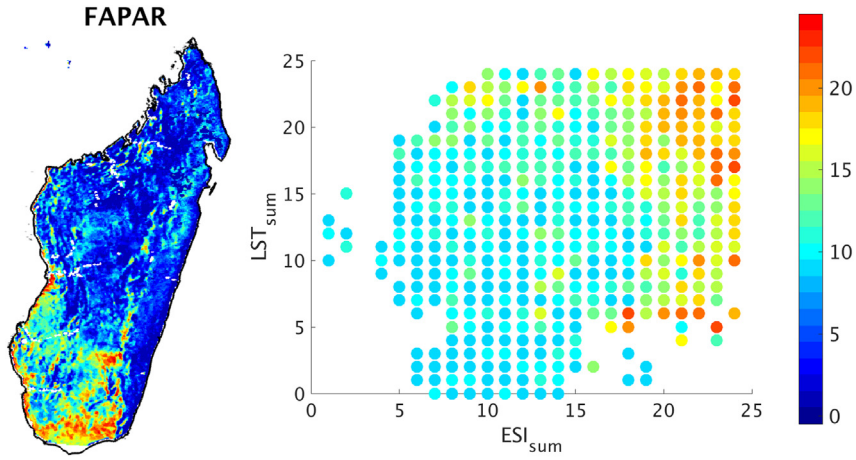

Figure 10. Number of months showing vegetative stress and its relation to hot and dry extremes

Left: spatial distribution of the number of months with FAPAR anomalies lower than −0.03 (middle) over Madagascar for the two years of 2020–2021. Right: scatterplot of prolonged dry (ESIsum) and hot (LSTsum) pixels for the pixels with more than nine months of negative anomalies of FAPAR. The color represents the number of months with negative impacts on vegetation (FAPARsum).

(2) The spatial-temporal link between vegetation conditions and droughts and hot events shows different characteristics, among which this link is more intense in the southern sectors of Madagascar than in the eastern and northern sectors.
(3) The compound dry-hot events are closely related to vegetation vulnerability during the wet seasons, although dry seasons are also affected. The cooccurrence seem to be intensified by the magnitude of the events.

The quantitative assessment of the cooccurrence of climatic and weather extreme events and vegetation conditions is of crucial importance for understanding the response of terrestrial ecosystems to climate change. Therefore, these results provide important insights into the response mechanism of ecosystems to compound extremes, which should be accounted for effective ecosystem management under future climate conditions in a particularly sensitive area like Madagascar, which already is facing a food security problem.

STAR★METHODS

Detailed methods are provided in the online version of this paper and include the following:

- KEY RESOURCES TABLE
- RESOURCE AVAILABILITY
  - Lead contact
  - Materials availability
  - Data and code availability
- METHOD DETAILS
  - Study area
  - Satellite data and methods

ACKNOWLEDGMENTS

This study was performed within the framework of the LSA-SAF, cofunded by EUMETSAT. All authors are grateful to Fundação para a Ciência e a Tecnologia, FCT I.P./MCTES for the national funding (PIDDAC)"—UIDB/50019/2020. A.R. and C.M.G. are grateful to project DHEFEUS (https://doi.org/10.54499/2022.09185.PTDC). A.R. is supported by the FCT through national funds from the MCTES within the Faculty of Sciences, University of Lisbon, through 2022.01167.CEECIND.

AUTHOR CONTRIBUTIONS

C.M.G. made the conceptual design of the study and defined the datasets to be used for the study. M.S. prepared the satellite datasets and computed the monthly values for the different variables. C.M.G. and A.R. participated in the interpretation and the redaction of the manuscript. C.M.G. and A.R. defined the approach used for the analysis. Each of the co-authors performed a thorough revision of the manuscript, provided useful advice on the intellectual content, and improved the English language.

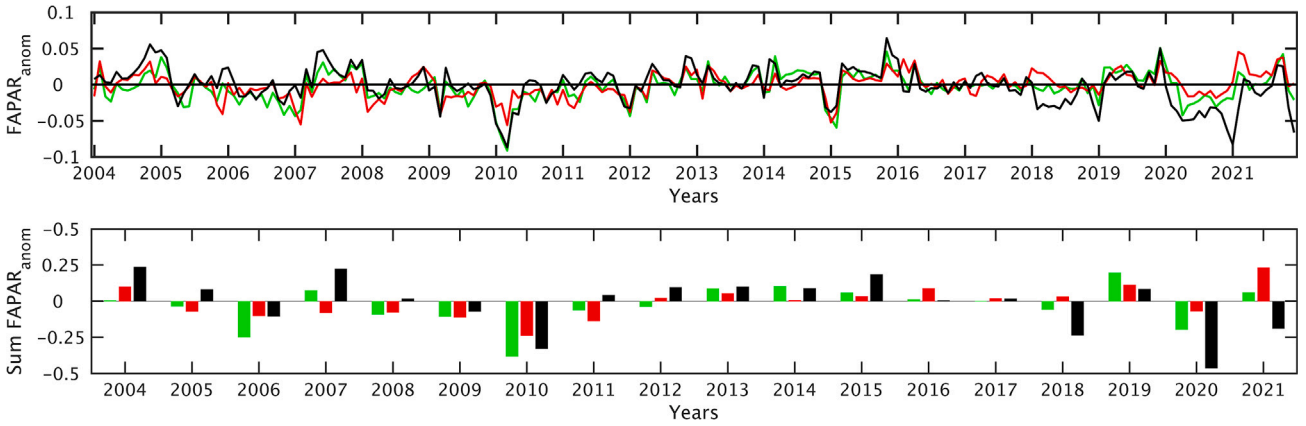

Figure 11. Temporal evolution of FAPAR anomaly values (top panel) and annual sums of FAPAR anomaly values (bottom panel) averaged over dry (green), hot (red), and hot and dry (black) pixels

DECLARATION OF INTERESTS

The authors declare that they have no known competing financial interests or personal relationships that could have appeared to influence the work reported in this paper.

Received: January 4, 2023
Revised: June 1, 2023
Accepted: December 4, 2023
Published: December 7, 2023

REFERENCES

1. UNDP (United Nations Development Programme) (2022). Human Development Report 2021-22: Uncertain Times, Unsettled Lives: Shaping Our Future in a Transforming World. https://hdr.undp.org/data-center/country-insights#/ranks.
2. Eckstein, D., Künzel, V., Schäfer, L., and Winges, M. (2018). GLOBAL CLIMATE RISK INDEX 2020. Who Suffers Most from Extreme Weather Events? Weather-Related Loss Events in 2018 and 1999 to 2018.
3. OCHA (UN Office for the Coordination of Humanitarian Affairs) (2022). FLASH APPEAL MADAGASCAR Grand Sud and Grand-Sudest, Report. https://reliefweb.int/report/madagascar/madagascar-grand-sud-and-grand-sud-est-flash-appeal-january-2021-december-2022-revised-june-2022.
4. Gouveia, C.M., Bastos, A., Trigo, R.M., and DaCamara, C.C. (2012). Drought Impacts on Vegetation in the Pre- and Post-Fire Events over Iberian Peninsula. Nat. Hazards Earth Syst. Sci. *12*, 3123–3137.
5. Gouveia, C.M., Bistinas, I., Liberato, M.L.R., Bastos, A., Koutsias, N., and Trigo, R.M. (2016). The Outstanding Synergy between Drought, Heatwaves and Fuel on the 2007 Southern Greece Exceptional Fire Season. In *Agricultural and Forest Meteorology*; Agricultural and Forest Meteorology (Elsevier Science B.V.), pp. 135–145.
6. Gouveia, C.M., Trigo, R.M., Beguería, S., and Vicente-Serrano, S.M. (2017). Drought Impacts on Vegetation Activity in the Mediterranean Region: An Assessment Using Remote Sensing Data and Multi-Scale Drought Indicators. Global Planet. Change *151*, 15–27.
7. Desbureaux, S., and Damania, R. (2018). Rain, forests and farmers: Evidence of drought induced deforestation in Madagascar and its consequences for biodiversity conservation. Biol. Conserv. *221*, 357–364.
8. Turco, M., Jerez, S., Augusto, S., Tarín-Carrasco, P., Ratola, N., Jiménez-Guerrero, P., and Trigo, R.M. (2019). Climate Drivers of the 2017 Devastating Fires in Portugal. Sci. Rep. *9*, 13886.
9. Vicente-Serrano, S.M., McVicar, T.R., Miralles, D.G., Yang, Y., and Tomas-Burguera, M. (2020). Unraveling the Influence of Atmospheric Evaporative Demand on Drought and Its Response to Climate Change. WIREs Climate Change *11*, e632.
10. Zhang, Y., Keenan, T.F., and Zhou, S. (2021). Exacerbated Drought Impacts on Global Ecosystems Due to Structural Overshoot. Nat. Ecol. Evol. *5*, 1490–1498.
11. WFP (2021). World Food Programme Madagascar 2021 Annual Country Report Highlights. https://www.wfp.org/publications/world-food-programme-madagascar-2021-annual-country-report-highlights.
12. Amnesty International (2021). https://www.amnesty.org/en/latest/news/2021/05/madagascar-urgent-humanitarian-intervention-needed-as-millions-face-hunger-due-to-devastating-famine/.
13. Barimalala, R., Raholijao, N., Pokam, W., and Reason, C.J.C. (2021). Potential impacts of 1.5° C, 2° C global warming levels on temperature and rainfall over Madagascar. Environ. Res. Lett. *16*, 044019.
14. Dyoulgerov, M. (2011). Climate Risk and Adaptation Country Profile: Madagascar (The World Bank Group).
15. IPCC (2021). Summary for Policymakers. In Climate Change 2021: The Physical Science Basis. Contribution of Working Group I to the Sixth Assessment Report of the Intergovernmental Panel on Climate Change, V. Masson-Delmotte, P. Zhai, A. Pirani, S.L. Connors, C. Péan, S. Berger, N. Caud, Y. Chen, L. Goldfarb, M.I. Gomis, and M. Huang, eds. (Cambridge University Press). https://www.smithschool.ox.ac.uk/sites/default/files/2022-03/ICC_report_final-sept-2021.pdf.
16. Mueller, B., and Seneviratne, S.I. (2012). Hot Days Induced by Precipitation Deficits at the Global Scale. Proc. Natl. Acad. Sci. USA *109*, 12398–12403.
17. Liu, X., Tang, Q., Liu, W., Yang, H., Groisman, P., Leng, G., Ciais, P., Zhang, X., and Sun, S. (2019). The Asymmetric Impact of Abundant Preceding Rainfall on Heat Stress in Low Latitudes. Environ. Res. Lett. *14*, 044010.
18. Russo, A., Gouveia, C.M., Dutra, E., Soares, P.M.M., Trigo, R.M., and Trigo. (2019). The Synergy between Drought and Extremely Hot Summers in the Mediterranean. Environ. Res. Lett. *14*, 014011.
19. Ribeiro, A.F., Russo, A., Gouveia, C.M., and Pires, C.A. (2020a). Drought-Related Hot Summers: A Joint Probability Analysis in the Iberian Peninsula. Weather Clim. Extrem. *30*, 100279.

20. Geirinhas, J.L., Russo, A., Libonati, R., Sousa, P.M., Miralles, D.G., and Trigo, R.M. (2021). Recent Increasing Frequency of Compound Summer Drought and Heatwaves in Southeast Brazil. Environ. Res. Lett. *16*, 034036.
21. Hao, Z., Hao, F., Singh, V.P., and Ouyang, W. (2017). Quantitative Risk Assessment of the Effects of Drought on Extreme Temperature in Eastern China. JGR. Atmospheres *122*, 9050–9059.
22. Holmes, A., Rüdiger, C., Mueller, B., Hirschi, M., and Tapper, N. (2017). Variability of Soil Moisture Proxies and Hot Days across the Climate Regimes of Australia. Geophys. Res. Lett. *44*, 7265–7275.
23. Páscoa, P., Gouveia, C.M., Russo, A., and Ribeiro, A.F.S. (2022). Summer Hot Extremes and Antecedent Drought Conditions in Australia. Int. J. Climatol. *42*, 5487–5502.
24. Fischer, E.M., Seneviratne, S.I., Vidale, P.L., Lüthi, D., and Schär, C. (2007). Soil Moisture–Atmosphere Interactions during the 2003 European Summer Heat Wave. J. Clim. *20*, 5081–5099.
25. Bastos, A., Ciais, P., Friedlingstein, P., Sitch, S., Pongratz, J., Fan, L., Wigneron, J.P., Weber, U., Reichstein, M., Fu, Z., et al. (2020). Direct and Seasonal Legacy Effects of the 2018 Heat Wave and Drought on European Ecosystem Productivity. Sci. Adv. *6*, eaba2724.
26. Bastos, A., Orth, R., Reichstein, M., Ciais, P., Viovy, N., Zaehle, S., Anthoni, P., Arneth, A., Gentine, P., Joetzjer, E., et al. (2021). Vulnerability of European Ecosystems to Two Compound Dry and Hot Summers in 2018 and 2019. Earth Syst. Dyn. *12*, 1015–1035.
27. Ermitão, T., Gouveia, C.M., Bastos, A., and Russo, A.C. (2022). Interactions between Hot and Dry Fuel Conditions and Vegetation Dynamics in the 2017 Fire Season in Portugal. Environ. Res. Lett. *17*, 095009.
28. Ermitão, T., Gouveia, C.M., Bastos, A., and Russo, A.C. (2021). Vegetation Productivity Losses Linked to Mediterranean Hot and Dry Events. Rem. Sens. *13*, 4010.
29. Vogel, M.M., Orth, R., Cheruy, F., Hagemann, S., Lorenz, R., van den Hurk, B.J.J.M., and Seneviratne, S.I. (2017). Regional Amplification of Projected Changes in Extreme Temperatures Strongly Controlled by Soil Moisture-Temperature Feedbacks. Geophys. Res. Lett. *44*, 1511–1519.
30. Vicente-Serrano, S.M., Quiring, S.M., Peña-Gallardo, M., Yuan, S., and Domínguez-Castro, F. (2020). A Review of Environmental Droughts: Increased Risk under Global Warming? Earth Sci. Rev. *201*, 102953.
31. Guion, A., Turquety, S., Polcher, J., Pennel, R., Bastin, S., and Arsouze, T. (2022). Droughts and Heatwaves in the Western Mediterranean: Impact on Vegetation and Wildfires Using the Coupled WRF-ORCHIDEE Regional Model (RegIPSL). Clim. Dynam. *58*, 2881–2903.
32. Smith, M.D. (2011). An Ecological Perspective on Extreme Climatic Events: A Synthetic Definition and Framework to Guide Future Research. J. Ecol. *99*, 656–663.
33. Teuling, A.J., Seneviratne, S.I., Stöckli, R., Reichstein, M., Moors, E., Ciais, P., Luyssaert, S., Van Den Hurk, B., Ammann, C., Bernhofer, C., et al. (2010). Contrasting Response of European Forest and Grassland Energy Exchange to Heatwaves. Nat. Geosci. *3*, 722–727.
34. Peters, W., Bastos, A., Ciais, P., and Vermeulen, A. (2020). A Historical, Geographical and Ecological Perspective on the 2018 European Summer Drought. Philos. Trans. R. Soc. Lond. B Biol. Sci. *375*, 20190505.
35. Weber, T., Bowyer, P., Rechid, D., Pfeifer, S., Raffaele, F., Remedio, A.R., Jacob, D., and Teichmann, C. (2020). Analysis of compound climate extremes and exposed population in Africa under two different emission scenarios. Earth's Future *8*, e2019EF001473.
36. Ghazaryan, G., König, S., Rezaei, E., Siebert, S., and Dubovyk, O. (2020). Analysis of Drought Impact on Croplands from Global to Regional Scale: A Remote Sensing Approach. Rem. Sens. *12*, 4030.
37. Qu, C., Hao, X., and Qu, J.J. (2019). Monitoring Extreme Agricultural Drought over the Horn of Africa (HOA) Using Remote Sensing Measurements. Rem. Sens. *11*, 902.
38. Rojas, O., Vrieling, A., and Rembold, F. (2011). Assessing Drought Probability for Agricultural Areas in Africa with Coarse Resolution Remote Sensing Imagery. Rem. Sens. Environ. *115*, 343–352.
39. Zhang, X., Friedl, M.A., Schaaf, C.B., Strahler, A.H., and Liu, Z. (2005). Monitoring the Response of Vegetation Phenology to Precipitation in Africa by Coupling MODIS and TRMM Instruments. J. Geophys. Res. *110*.
40. Mazdiyasni, O., and AghaKouchak, A. (2015). Substantial Increase in Concurrent Droughts and Heatwaves in the United States. Proc. Natl. Acad. Sci. USA *112*, 11484–11489.
41. Sharma, S., and Mujumdar, P. (2017). Increasing Frequency and Spatial Extent of Concurrent Meteorological Droughts and Heatwaves in India. Sci. Rep. *7*, 15582.
42. Langenbrunner, B. (2021). Water, Water Not Everywhere. Nat. Clim. Change *11*, 650.
43. Makoni, M. (2021). Southern Madagascar Faces "Shocking" Lack of Food. Lancet *397*, 2239.
44. Carbon Brief (2022). Mapped: How Climate Change Affects Extreme Weather Around the World. https://www.carbonbrief.org/mapped-how-climate-change-affects-extreme-weather-around-the-world/.
45. Lobell, D.B., Sibley, A., and Ivan Ortiz-Monasterio, J. (2012). Extreme Heat Effects on Wheat Senescence in India. Nat. Clim. Change *2*, 186–189.
46. Flower, C.E., and Gonzàlez-Meler, M. (2015). Responses of Temperate Forest Productivity to Insect and Pathogen Disturbances. Annu. Rev. Plant Biol. *66*, 547–569.
47. Profile, M.C. (2016). Madagascar (World Health Organization).
48. Trigo, I.F., Dacamara, C.C., Viterbo, P., Roujean, J.-L., Olesen, F., Barroso, C., Camacho-de-Coca, F., Carrer, D., Freitas, S.C., García-Haro, J., et al. (2011). The Satellite Application Facility for Land Surface Analysis. Int. J. Rem. Sens. *32*, 2725–2744.
49. Gouveia, C.M., Martins, J.P.A., Russo, A., Durão, R., and Trigo, I.F. (2022). Monitoring Heat Extremes across Central Europe Using Land Surface Temperature Data Records from SEVIRI/MSG. Rem. Sens. *14*, 3470.
50. Gouveia, C., Trigo, R.M., and DaCamara, C.C. (2009). Drought and Vegetation Stress Monitoring in Portugal Using Satellite Data. Nat. Hazards Earth Syst. Sci. *9*, 185–195.
51. Gouveia, C., Trigo, R.M., DaCamara, C.C., Libonati, R., and Pereira, J.M.C. (2008). The North Atlantic Oscillation and European Vegetation Dynamics. Int. J. Climatol. *28*, 1835–1847.
52. Trigo, I.F., Ermida, S.L., Martins, J.P., Gouveia, C.M., Göttsche, F.M., and Freitas, S.C. (2021). Validation and Consistency Assessment of Land Surface Temperature from Geostationary and Polar Orbit Platforms: SEVIRI/MSG and AVHRR/Metop. ISPRS J. Photogrammetry Remote Sens. *175*, 282–297.
53. Freitas, S.C., Trigo, I.F., Bioucas-Dias, J.M., and Gottsche, F.-M. (2010). Quantifying the Uncertainty of Land Surface Temperature Retrievals From SEVIRI/Meteosat. IEEE Trans. Geosci. Rem. Sens. *48*, 523–534.
54. LSA-SAF (2016). Algorithm Theoretical Basis Document for Vegetation Parameters (VEGA). Ref: SAF/LAND/UV/ATBD_VEGA/2.0https://landsaf.ipma.pt.
55. Roujean, J.-L., and Breon, F.-M. (1995). Estimating PAR Absorbed by Vegetation from Bidirectional Reflectance Measurements. Rem. Sens. Environ. *51*, 375–384.
56. LSA-SAF (2018). Validation Report for Vegetation Parameters (VEGA). Ref: SAF/LAND/UV/VR_VEGA_MSG/3.1. https://landsaf.ipma.pt.
57. de Bruin, H.A.R., Trigo, I.F., Bosveld, F.C., and Meirink, J.F. (2016). A Thermodynamically Based Model for Actual Evapotranspiration of an Extensive Grass Field Close to FAO Reference, Suitable for Remote Sensing Application. J. Hydrometeorol. *17*, 1373–1382.
58. Trigo, I.F., de Bruin, H., Beyrich, F., Bosveld, F.C., Gavilán, P., Groh, J., and López-Urrea, R. (2018). Validation of Reference Evapotranspiration from Meteosat Second Generation (MSG) Observations. Agric. For. Meteorol. *259*, 271–285.
59. Barrios, J., Arboleda, A., and Gellens-Meulenberghs, F. (2021). Remote Sensing of Evapotranspiration and Surface Heat Fluxes in the LSA-SAF Programme. In 2021 IEEE International Geoscience and Remote Sensing Symposium (IEEE IGARSS 2021)), pp. 6873–6876.
60. Anderson, M.C., Norman, J.M., Mecikalski, J.R., Otkin, J.A., and Kustas, W.P. (2007). A Climatological Study of Evapotranspiration and Moisture Stress across the Continental United States Based on Thermal Remote Sensing: 2. Surface Moisture Climatology. J. Geophys. Res. *112*, D11112.
61. Anderson, M.C., Norman, J.M., Mecikalski, J.R., Otkin, J.A., Kustas, W.P., Anderson, C., Norman, J., Mecikalski, J., Otkin, J., and Kustas, W. (2007). A Climatological Study of Evapotranspiration and Moisture Stress across the Continental United States Based on Thermal Remote Sensing: 1. Model Formulation. J. Geophys. Res. *112*.
62. Anderson, M.C., Hain, C., Wardlow, B., Pimstein, A., Mecikalski, J.R., and Kustas, W.P. (2011). Evaluation of Drought Indices Based on Thermal Remote Sensing of Evapotranspiration over the Continental United States. J. Clim. *24*, 2025–2044.
63. Anderson, M.C., Norman, J.M., Mecikalski, J.R., Otkin, J.A., and Kustas, W.P. (2007). A Climatological Study of Evapotranspiration and Moisture Stress across the Continental United States Based on Thermal Remote Sensing: 2. Surface Moisture Climatology. J. Geophys. Res. *112*.
64. McEvoy, D.J., Huntington, J.L., Hobbins, M.T., Wood, A., Morton, C., Anderson, M., and Hain, C. (2016). The Evaporative Demand Drought Index. Part II: CONUS-Wide Assessment against Common Drought Indicators. J. Hydrometeorol. *17*, 1763–1779.
65. Anderson, M.C., Zolin, C.A., Sentelhas, P.C., Hain, C.R., Semmens, K., Tugrul Yilmaz, M.,

Gao, F., Otkin, J.A., and Tetrault, R. (2016). The Evaporative Stress Index as an Indicator of Agricultural Drought in Brazil: An Assessment Based on Crop Yield Impacts. Rem. Sens. Environ. *174*, 82–99.

66. Lee, H.-J., Nam, W.-H., Yoon, D.-H., Hong, E.-M., Kim, D.-E., Svoboda, M.D., and Wardlow, T.T.B.D. (2019). Satellite-based Evaporative Stress Index (ESI) as an Indicator of Agricultural Drought in North Korea. Journal of The Korean Society of Agricultural Engineers *61*, 1–14.
67. Lee, H.-J., Nam, W.-H., Yoon, D.-H., Hong, E.-M., Kim, T., Park, J.-H., and Kim, D.-E. (2020). Percentile Approach of Drought Severity Classification in Evaporative Stress Index for South Korea. Journal of The Korean Society of Agricultural Engineers *62*, 63–73.
68. Nguyen, H., Wheeler, M.C., Otkin, J.A., Cowan, T., Frost, A., and Stone, R. (2019). Using the Evaporative Stress Index to Monitor Flash Drought in Australia. Environ. Res. Lett. *14*, 064016.
69. Zhan, X., Fang, L., Yin, J., Schull, M., Liu, J., Hain, C., Anderson, M., Kustas, W., and Kalluri, S. (2021). Remote Sensing of Evapotranspiration for Global Drought Monitoring. In Global Drought and Flood (American Geophysical Union (AGU)), pp. *29*–46.
70. Zscheischler, J., and Seneviratne, S.I. (2017). Dependence of drivers affects risks associated with compound events. Sci. Adv. *3*, e1700263.
71. Zscheischler, J., Westra, S., van den Hurk, B.J.J.M., Seneviratne, S.I., Ward, P.J., Pitman, A., AghaKouchak, A., Bresch, D.N., Leonard, M., Wahl, T., and Zhang, X. (2018). Future climate risk from compound events. Nat. Clim. Change *8*, 469–477.
72. AghaKouchak, A., Chiang, F., Huning, L.S., Love, C.A., Mallakpour, I., Mazdiyasni, O., Moftakhari, H., Papalexiou, S.M., Ragno, E., and Sadegh, M. (2020). Climate Extremes and Compound Hazards in a Warming World. Annu. Rev. Earth Planet Sci. *48*, 519–548.
73. Sutanto, S.J., Vitolo, C., Di Napoli, C., D'Andrea, M., and Van Lanen, H.A.J. (2020). Heatwaves, droughts, and fires: Exploring compound and cascading dry hazards at the pan-European scale. Environ. Int. *134*, 105276.
74. Rammig, A., Wiedermann, M., Donges, J.F., Babst, F., von Bloh, W., Frank, D., Thonicke, K., and Mahecha, M.D. (2015). Coincidences of climate extremes and anomalous vegetation responses: comparing tree ring patterns to simulated productivity. Biogeosciences *12*, 373–385.
75. Wu, X., Hao, Z., Hao, F., Li, C., and Zhang, X. (2019). Spatial and temporal variations of compound droughts and hot extremes in China. Atmosphere *10*, 95.
76. Ribeiro, A.F.S., Russo, A., Gouveia, C.M., Páscoa, P., and Zscheischler, J. (2020b). Risk of crop failure due to compound dry and hot extremes estimated with nested copulas. Biogeosciences *17*, 4815–4830.
77. Miralles, D.G., Gentine, P., Seneviratne, S.I., and Teuling, A.J. (2019). Land-Atmospheric Feedbacks during Droughts and Heatwaves: State of the Science and Current Challenges. Ann. N. Y. Acad. Sci. *1436*, 19–35.
78. Zhao, T., and Dai, A. (2015). The magnitude and causes of global drought changes in the twenty-first century under a low–moderate emissions scenario. J. Clim. *28*, 4490–4512.
79. Hao, Z., and AghaKouchak, A. (2013). Multivariate standardized drought index: a parametric multi-index model. Adv. Water Resour. *57*, 12–18.
80. Okpara, J.N., Ogunjobi, K.O., and Adefisan, E.A. (2022). Developing objective dry spell and drought triggers for drought monitoring in the Niger Basin of West Africa. Nat. Hazards *112*, 2465–2492.
81. Ionita, M., and Nagavciuc, V. (2021). Changes in drought features at the European level over the last 120 years. Nat. Hazards Earth Syst. Sci. *21*, 1685–1701.
82. Frank, D., Reichstein, M., Bahn, M., Thonicke, K., Frank, D., Mahecha, M.D., Smith, P., van der Velde, M., Vicca, S., Babst, F., et al. (2015). Effects of climate extremes on the terrestrial carbon cycle: concepts, processes and potential future impacts. Global Change Biol. *21*, 2861–2880.
83. Ye, C., Sun, J., Liu, M., Xiong, J., Zong, N., Hu, J., Huang, Y., Duan, X., and Tsunekawa, A. (2020). Concurrent and lagged effects of extreme drought induce net reduction in vegetation carbon uptake on Tibetan Plateau. Rem. Sens. *12*, 2347.
84. Wang, S., Zhang, Y., Ju, W., Porcar-Castell, A., Ye, S., Zhang, Z., Brümmer, C., Urbaniak, M., Mammarella, I., Juszczak, R., and Folkert Boersma, K. (2020). Warmer spring alleviated the impacts of 2018 European summer heatwave and drought on vegetation photosynthesis. Agric. For. Meteorol. *295*, 108195.

STAR★METHODS

KEY RESOURCES TABLE

REAGENT or RESOURCE	SOURCE	IDENTIFIER
Deposited data		
Land Surface Temperature	LSA-SAF	http://doi.org/10.15770/EUM_SAF_LSA_0001
Evapotranspiration	LSA-SAF	https://landsaf.ipma.pt/en/data/products/evapotranspiration-turbulent-fluxes/
Reference Evapotranspiration	LSA-SAF	https://landsaf.ipma.pt/en/data/products/evapotranspiration-turbulent-fluxes/
Fraction of Absorbed Photosynthetically Active Radiation	LSA-SAF	http://doi.org/10.15770/EUM_SAF_LSA_0005
ESA-CCI land cover product for 2018	ESA-CCI	http://maps.elie.ucl.ac.be/CCI/viewer/download.php

RESOURCE AVAILABILITY

Lead contact

Any additional information required to reanalyze the data reported in this paper is available from the lead contact upon request: C.M. Gouveia (celia.gouveia@ipma.pt).

Materials availability

This study did not generate new datasets.

Data and code availability

- This paper does not report original code.
- This paper analyzes existing, publicly available data. These accession numbers for the datasets are listed in the key resources table.
- Any additional information required to reanalyze the data reported in this paper is available from the lead contact upon request.

METHOD DETAILS

Study area

Madagascar is a large island in the Southwestern Indian Ocean located at the east of Mozambique. The highest peak is Maromokotro (2876 m) located in the Tsaratanana Massif region in the northern sector of the island (Figure 1A). The east coast is dominated by lowlands leading to sharp bluffs and central highland close to the center of the island. The capital is Antananarivo which is located in the central highland. The average elevation of Madagascar is around 440 m above. Many protected harbors and broad plains are located on the west coast and the southwestern region is a desert plateau.

The climate is arid in the south and tropical along the coast with temperate areas inland. The island has substantial freshwater resources and around 70% of the mainland is agricultural land that employs over 60% of the population. Irrigated rice cultivation occurs in river valleys and marshes and most of the agricultural land is inland, despite some forest and hillsides clearings for agricultural practices.[47] Madagascar climate is characterized by two seasons: a cool and dry season from May to October and a warm and wet season from November to April. Tropical rainforest climate dominates the east coast which is also exposed to the trade winds. The dense humid forest, located on the eastern slope of Madagascar, grows under wet conditions (Figure 1B). Due to the rain clouds discharging in the east mountains, the central highlands are drier and cooler. Grassland, woodland and dense dry forest occur across the central highlands and west coast, where the rainy season is shorter, from November to April (Figure 1B). The west coast is drier than the east coast or central highlands and the southwest and the extreme south are semi-desert regions. Cereal and legumes are commonly not irrigated crops in regions that are therefore very sensitive to drought conditions.[47]

Satellite data and methods

Data

Satellite Application Facility on Land Surface Analysis (LSA-SAF) project, which is part of the distributed EUMETSAT (European Organization for the Exploitation of Meteorological Satellites) Application Ground Segment, disseminates several products, namely the Fraction of Absorbed Photosynthetically Active Radiation (FAPAR), Land Surface Temperature (LST) and Reference (ETo) and Evapotranspiration

(ET).[48] The products, freely available (https://lsa-saf.eumetsat.int), are derived from Spinning Enhanced Visible and Infrared Imager (SEVIRI) onboard the geostationary satellite Meteosat Second Generation (MSG), with a maximum spatial resolution (at the sub-satellite point) of about 3 km at nadir point. MSG daily ETo, ET, FAPAR and 15-min LST products are operationally distributed in near real-time (NRT). However, the need for providing homogeneous time series of Climate Data Records (CDR) suitable for climate variability and change detection studies justified the generation of long-term datasets with the most recent algorithm version used for NRT operational products. The corresponding LST, ETo, and FAPAR CDRs (LSA-050, LSA-303, and LSA-452, respectively) have been available since 2017, covering the period between 2004 and 2015. Therefore, the available datasets, including reprocessed and operational NRT products, resulted in almost 19 years of satellite information, i.e., data from 2004 until the present. In this work data from 2004 to 2021 were used for the above-mentioned datasets.

The LST is controlled by the surface energy balance, which depends on the thermal properties of the surface and the atmosphere. LST and air temperature are conceptually distinct, although having a strong relationship between the two leads to LST often being used as a proxy for air temperature.[49] Satellite-based LST products also have the advantage of being available with high spatial resolution and coverage compared to meteorological *in situ* measurements.[49–51] The LST product within the LSA-SAF framework is based on the generalized split-window algorithm, using top-of-atmosphere brightness temperatures from the infrared at 10.8 and 12.0 μm. Further details on the algorithm and validation can be found in Trigo et al. ,[48,52] Freitas et al.,[53] or Gouveia et al.[49]

FAPAR corresponds to the fraction of photosynthetically active radiation (i.e., within 400–700 nm) absorbed by vegetation and quantifies the canopy's ability to absorb radiation for photosynthesis.[54] The FAPAR product is derived from SEVIRI red and NIR channels, using information on the surface bidirectional reflectance distribution function (BRDF).[55] Details about the LSA-SAF FAPAR algorithm (MTFAPAR) and validation are available at LSA-SAF.[54,56] FAPAR was also reprocessed using the most recent version VEGAv3.0 algorithm with daily and 10-day temporal resolution.

ETo is defined as the evapotranspiration rate from a clearly defined reference surface. ETo quantifies, under a situation with a certain downwelling shortwave radiation, the evapotranspiration from a theoretical well-watered green grass field with 12 cm height and with an albedo of 0.23.[57] The ETo product derived from SEVIRI and disseminated operationally by the LSA SAF (METREF) with a daily temporal sampling, aims to quantify the evaporative demand of the atmosphere independently of crop type, development, or management techniques. Further details on the algorithm and validation can be found in De Bruin et al.,[57] (2016) and Trigo et al.[58] ET accounts for the flux of water from the Earth's surface into the atmosphere. This flux results from water evaporation from a wide range of surfaces, such as shallow soil, water bodies, water in the vegetation canopy, and the transpiration of plants.[59] The algorithm includes information from long and short incoming solar radiation, albedo, leaf area index (LSA SAF) and soil moisture estimate from the SM-DAS-2 (H14, H-SAF). The recent post-processing ET CDR from 2004 to 2021 with a temporal sampling of 30 min,[59] used the most recent version of the algorithm and is intended to support analyses of trends and anomalies in ET and surface fluxes over spatial domains within the MSG field of view. Results from the validation exercises comparing ET using *in situ* energy flux measurements, the reprocessed dataset and further details will be available very soon on the LSA-SAF website.

The land cover map from ESA-CCI land cover product for 2018 was here used. Each pixel in this land cover corresponds to a land cover class defined based on the UN Land Cover Classification System (LCCS) and counts 22 global land cover categories. The land cover maps until 2015 (v207) were generated within the framework of the ESA-CCI and from 2016 to present date, they are operationally generated under the EC Copernicus Climate Change Service. The land cover classification for Madagascar was extracted from ESA-CCI Viewer (http://maps.elie.ucl.ac.be/CCI/viewer/download.php) (Figure 1B).

Recently, the ratio of ET to ETo, known as the Evaporative Stress Index (ESI), has been used as a drought indicator that accounts for feedback at the interface between land surface and atmosphere.[60–64] The ESI has proved to provide early warning of the rapid onset of drought development, as it is very sensitive to rapid changes in soil moisture, driven by changes in air temperature, wind speed, specific humidity and downwelling shortwave radiation.[63] The ESI has been used to monitor droughts and flash droughts in Brazil, Australia, and South and North Corea,[65,66,67,68] and is currently used for monitoring drought for North America.[69]

Compound approaches

Nowadays there is strong evidence that natural hazards are at times synergetic (e.g.,[16–23]) and that their combined occurrence has aggravated impacts,[70–72] but conventional risk assessment approaches only contemplate single hazards.[73] Moreover, as climate change progresses, there is a need for additional knowledge and understanding of the interactions and interdependence of natural hazards because some of the key drivers are changing rapidly.[70]

Concurrent and amplified drought and heatwave events can strongly affect vegetation health, prompting tree mortality and favoring fires,[5,72] which can cause wide-ranging societal problems. Nevertheless, the underlying mechanisms associated with the chain of events encompassing droughts, heatwaves, and vegetation changes are still not fully understood. Multidimensional effects need to be considered in estimating both climate and vegetation effects to deliver public administrators effective early warning tools.

Recent studies have characterized compound events based on distinct statistical approaches, including event coincidence analysis,[27,28,74] frequency of simultaneous occurrences of multiple extremes,[75] or copula analyses2020b).[19,70,76] Despite the scientific progress to date, the full comprehension of the mechanistic links associated with compound events is in its early stages.[19] Conceptual and technical barriers remain, such as the ambiguity in drought and heatwave definitions, limitations of data products, and challenges in the characterization of causal links across the land–atmosphere interplay.[19,77]

Methodological approach

The available LST dataset, considered here for the total 2004–2021 period, was post-processed to obtain monthly mean values from the original 15-min values, taking into account the representativeness of the LST diurnal cycle. The available ET0, ET and FAPAR datasets were post-processed to obtain monthly mean values from the original daily data. Monthly LST, ET, ETo and FAPAR fields are computed considering the reference period from 2004 to 2021. Monthly fields of ESI, computed as the ratio of ET/ETo are also calculated for the same period. The monthly anomalies were obtained as the departures from the monthly means for the entire considered period.

Following the methodology defined in Gouveia et al.,[49,50] the persistency of dry and hot climate extremes for the two consecutive years period of 2020–2021 is evaluated considering, respectively, the persistence of anomalies of ESI below and under the 20th percentile and anomalies of LST above the 80th percentile. The impacts of the isolated and composite hot and dry conditions on vegetation activity are assessed through the FAPAR anomaly values below the 20th percentile during the long-lasting duration of the events. The value of the percentiles 20 to define moderate drought and vegetative stress is in accordance to several previous works.[78–81] Following the same rationale, the percentile 80 is used to define moderate hot extremes respectively. Therefore, the number of months with LST anomalies higher than 1°C (80^{th} percentile), ESI anomalies lower than −0.05 (20^{th} percentile), and FAPAR anomalies lower than −0.03 (20^{th} percentile) for the two years of 2020–2021 are computed for the 2-years period of 2020–2021, over the Madagascar Island.

In order to evaluate the isolated and compound impacts of hot and dry extremes on vegetation activity the pixels with more than 9 months in vegetative stress (i.e., with monthly anomaly values lower than the 20th percentile) were selected. The threshold of 9 was chosen following the approach used to define moderate climate extremes (i.e., using the 20^{th} and 80^{th} percentiles) in this case, applicable to the growing season of the two considered years. The wet season duration in Madagascar is around 6 months and the option of considering regions with vegetation showing 9 months of stress means that more than two-thirds of the wet season months (12 months) exhibited vegetative stress conditions. Several thresholds were tested, and the results are very consistent. However, the threshold of 9 months was selected as revealed to be a good compromise between the number of months with negative anomalies of ESI and positive anomalies of LST. Moreover, the choice of more than 9 months in vegetative stress corresponds to approximately 20% of the island affected (Table 1), being consistent with the previous assumptions. The sum of months showing dry and hot extremes was evaluated for the pixels showing more than 9 months with vegetative stress. The temporal evolution of FAPAR monthly anomaly values over the pixels showing heat or dry conditions and pixels showing hot and dry conditions during the 2-years period is also analyzed. It should be stressed that the simultaneous or cascading occurrence of dry, hot and vegetation stress conditions do not require the co-occurrence in the same month, but the happening of such extremes in the considered period of 2 years[82–84]